Forced Assembly of Polymer Nanolayers Thinner Than the Interphase

R. Y. F. Liu,† A. P. Ranade, H. P. Wang, T. E. Bernal-Lara,‡ A. Hiltner,* and E. Baer

Department of Macromolecular Science, and Center for Applied Polymer Research, Case Western Reserve University, Cleveland, Ohio 44106-7202

Received July 26, 2005; Revised Manuscript Received October 5, 2005

ABSTRACT: When two polymers are brought into intimate contact, the interface is not perfectly sharp. Instead, localized molecular mixing produces an interphase with thickness on the order of 10 nm. Forced assembly by layer multiplying coextrusion makes it possible to create films that are entirely interphase. The new interphase materials can be characterized using conventional tools of polymer analysis. In this study we vary the ratio of poly(methyl methacrylate) (PMMA) to polycarbonate (PC) in the coextrusion process in order to obtain very thin PMMA nanolayers sandwiched between thicker (∼50 nm) PC layers. We use oxygen permeability to probe the nature of the interphase as the PMMA layer thickness is reduced below the interphase thickness to the limit of layer stability. If the PMMA nanolayers are made thinner than the 12 nm interphase dimension, they more closely resemble a thin interphase region sandwiched between thicker PC layers than they do discrete PMMA layers. The interphase region becomes progressively thinner with decreasing PMMA layer thickness until the limit in melt stability of the PMMA layer is reached. Efforts to obtain PMMA nanolayers thinner than 5 nm resulted in layer instability and breakup. Oxygen permeability suggested that the nanolayer fragments had a very high aspect ratio.

Introduction

Forced assembly of two dissimilar polymers using layer multiplying coextrusion makes it possible to fabricate films with thousands of alternating layers. The thickness of an individual nanolayer can be on the size scale of the polymer interphase.[1,2] The high fraction of interphase makes it possible to probe the interphase with conventional tools of polymer analysis. Previous studies utilized the 50/50 (v/v) composition to examine the effect of layer thickness on the glass transition behavior and the oxygen permeability.[3] Decreasing the layer thickness gradually revealed the effect of interfacial molecular mixing until the layers were thin enough that the film was a completely new material that was entirely interphase. Analysis of the layer thickness effect according to a three-layer interphase model provided a quantitative determination of the interphase thickness. By combining many pairs of immiscible amorphous polymers, it was demonstrated that the interphase thickness and interphase strength depended on interaction strength in accordance with model predictions based on the χ parameter.[4,5]

The previous studies utilized exclusively forced assemblies with the 50/50 (v/v) composition. Although this was the optimum condition for characterizing the interphase, achieving a layer thickness on the nanoscale required forced assembly of thousands of layers. Consequently, the process imposed a practical limit in layer thickness of 5−10 nm. However, by changing the composition ratio in the coextrusion process, it is possible to fabricate assemblies with very thin layers of one constituent sandwiched between thicker layers of the other constituent. With this approach, the achievable nanolayer thickness should be limited only by the stability of the nanolayer in the melt. The utility of this approach was demonstrated recently with thin polypropylene or polyethylene nanolayers confined between thick polystyrene layers.[6,7]

It is the purpose of this study to probe the interphase between PMMA and PC as the PMMA layer thickness is reduced to the limit of layer stability. If the PMMA layer is thinner than the 10 nm interphase dimension reported for this polymer pair,[3] the very thin PMMA layer more closely resembles an interphase layer between thick PC layers than it does a discrete PMMA layer. It is not clear what will happen when the PMMA layer is made much thinner than the equilibrium dimension of the interphase. At least two possibilities are imagined. The interphase thickness can decrease in parallel with the PMMA layer thickness and become thinner than 10 nm. Alternatively, the thickness of the interphase can be maintained and the fraction of PMMA in the interphase can decrease. Distinguishing between these possibilities is one goal of the present study.

Materials and Methods

Poly(methyl methacrylate) (PMMA) was provided by Atofina Chemicals, Inc. (Plexiglas V826, M_w = 132 kg mol^{-1}), and polycarbonate (PC) was provided by The Dow Chemical Co. (Calibre 200-14, MFI = 14). Films with many alternating PMMA and PC layers were fabricated using the layer-multiplication process described previously.[8,9] The extruder temperatures of 270 °C for PMMA and 290 °C for PC were chosen to ensure matching viscosities when the polymer melts were combined in the feedblock. Films with 2048 layers were created with an assembly of 10 multiplying elements. The layered melt was spread in a film die to achieve target film thicknesses of 50 and 100 μm. The temperature of the layer multipliers and film die was 280 °C. Rapid quenching on a chill roll equipped with an air knife froze the interfacial morphology. The feed ratio was varied in order to obtain PMMA nanolayers sandwiched between thicker PC layers. In addition, a 75 μm thick film with 512 layers and 50/50 (v/v) composition was coextruded to obtain layers that were thicker than 100 nm and therefore thick enough that the effect of the interphase was negligible.[3] Control PC and PMMA films were obtained by coextrusion with the constituent polymer in both extruders. Control films of various thicknesses were extruded

† Present address: 3M, St. Paul, MN 55144.
‡ Present address: The Dow Chemical Company, Freeport, TX 77541.
* Corresponding author: e-mail: ahiltner@case.edu.

10.1021/ma051649x CCC: $30.25
Published on Web 11/19/2005

Table 1. Oxygen Permeability of PC and PMMA Control Films

material	no. of layers	approximate film thickness (μm)	density (g/cm^3)	oxygen permeability[a]
PC	8	125	1.1938	9.89 ± 0.02
PC	32	50	1.1934	9.91
PC	2048	50	1.1936	9.90 ± 0.3
PMMA	8	125	1.1934	0.351 ± 0.001
PMMA	32	50	1.1923	0.371
PMMA	2048	50	1.1933	0.373 ± 0.04
PMMA	2048	100	1.1933	0.367 ± 0.001

[a] Permeability in cm^3 (STP) cm m^{-2} day^{-1} atm^{-1}.

with 8 (2 multipliers), 32 (4 multipliers), and 2048 layers (Table 1).

The feed ratio in the coextrusion process, especially if controlled by metering pumps, generally gives an accurate measure of film composition.[3−5] Therefore, the nominal layer thicknesses $d_{0,PMMA}$ and $d_{0,PC}$ calculated from the number of layers, the feed ratio, and the film thickness were considered reliable (Table 2). However, the film composition was confirmed independently by refractive index and infrared spectroscopy. Refractive index (RI) of the films was measured at 23 °C using a Metricon 2010 prism coupler equipped with a 632.8 nm laser. Infrared spectra of the films were collected by photoacoustic Fourier transform infrared (FTIR) spectroscopy at ambient temperature with a Nicolet 870 FTIR spectrometer using a MTEC model 200 photoacoustic cell. The spectral resolution was 4 cm^{-1}, and 128 scans were collected for each specimen. Both refractive index and infrared spectroscopy methods suggested that films with nominally 99/1, 98/2, and 97/3 (PC/PMMA) composition based on the melt flow rate were slightly higher than expected in PMMA (Table 2). Subsequent analysis of these films was based on the composition from refractive index measurements. Infrared and refractive index measurements on films with higher PMMA content confirmed the composition from melt flow rate within the <0.2% uncertainty of the measurements.

For atomic force microscopy (AFM), films were embedded in epoxy and sectioned perpendicular to the plane of the film and perpendicular to the extrusion direction as described previously.[4,5] Phase and height images of the cross section were recorded simultaneously using the tapping mode of the Nanoscope IIIa MultiMode scanning probe.

Oxygen permeability was measured using an OXTRAN 2/20 unit. The detailed procedure was described previously.[10] The maximum accumulated error from the instrument, the preparation and handling of identical specimens, and the curve fitting is estimated to be 3%.

Results

Layer Characterization. The close modulus match between PMMA and PC resulted in relatively poor contrast in AFM phase images. Nevertheless, if the nominal PMMA layer thickness was at least 10 nm, continuous dark layers of PMMA separated by thicker, light layers of PC were easily resolved (Figure 1a). A continuous layered texture was observed in films with $d_{0,PMMA}$ as thin as 5 nm (Figure 1b). The fine layered texture that could be discerned between the occasional brighter layers in the phase image had a spacing that corresponded to the sum of $d_{0,PMMA}$ and $d_{0,PC}$. The PC/PMMA interphase thickness is reported to be about 10 nm, which is thicker than the PMMA layers. Thus, the very thin PMMA layers more closely resembled interphase layers between thicker PC layers than they did discrete PMMA layers. The thin interphase layers that separated and defined the thicker PC layers were not resolved well enough to measure their thickness. Because of the close modulus match between PC and PMMA, phase contrast was lost in higher resolution images.

If surface-tension-driven breakup of PMMA layers had occurred, it would have been readily apparent as layer thickening, discontinuous layers, and even particle formation. Indeed, discontinuous PMMA layers were observed in films with $d_{0,PMMA}$ of 3.28 nm or less (Figure 1c). Thickening due to retraction of the broken layers resulted in measured PMMA layer thickness in the range of 30 nm, which was much larger than the nominal thickness. Additionally, the spacing between

Table 2. Characteristics of PC/PMMA Films with 2048 Layers

composition PC/PMMA	film thickness (μm)	$d_{0,PMMA}$ (nm)	$d_{0,PC}$ (nm)	P[a]	d_{PMMA} (nm)	d_I (nm)	P'	P''	α
				$d_{0,PMMA} < d_I$					
100/0	52			9.90 ± 0.03					
98.3/1.7[b]	56	0.93	54	7.98 ± 0.05					26
97.5/2.5[b]	57	1.39	54	6.59 ± 0.12					37
96.9/3.1[b]	57	1.73	54	6.34 ± 0.20					33
96/4	54	2.11	51	6.38 ± 0.09					24
95/5	56	2.73	52	5.90 ± 0.05					24
94/6	56	3.28	51	6.01 ± 0.05					18
90/10	52	5.08	46	4.99	−0.13	5.20	6.41	4.90	
95/5	114	5.57	106	6.36 ± 0.15	0.33	5.24	7.71	6.55	
87/13	51	6.47	43	4.12	0.24	6.23	5.51	4.24	
85/15	54	7.91	45	3.65	0.62	7.29	4.84	3.90	
92/8	104	8.13	93	5.34 ± 0.06	0.24	7.89	6.31	5.44	
80/20	51	10.0	40	3.03	0.72	9.24	3.69	3.25	
90/10	105	10.2	92	4.90 ± 0.10	−0.01	10.3	5.31	4.90	
				$d_{0,PMMA} \geq d_I$					
88/12	100	11.7	86	3.90	1.8	9.7			
70/30	49	14.4	33	1.89	3.6	10.7			
84/16	102	15.9	84	3.10	3.4	12.3			
82/18	100	17.6	80	2.47	7.3	10.1			
80/20	100	19.5	78	2.45 ± 0.02	6.1	13.2			
77/23	97	21.8	73	2.06	8.8	12.8			
75/25	91	22.2	67	1.87	9.9	12.1			
73/27	91	24.0	65	1.73	11.2	12.6			
70/30	99	29.0	68	1.50 ± 0.02	15.7	13.0			
50/50[c]	75	146	146	0.750					
0/100	51			0.373 ± 0.04					

[a] P = permeability in cm^3 (STP) cm m^{-2} day^{-1} atm^{-1}. [b] Nominally 99/1, 98/2, 97/3. Composition from RI. [c] 512 layers.

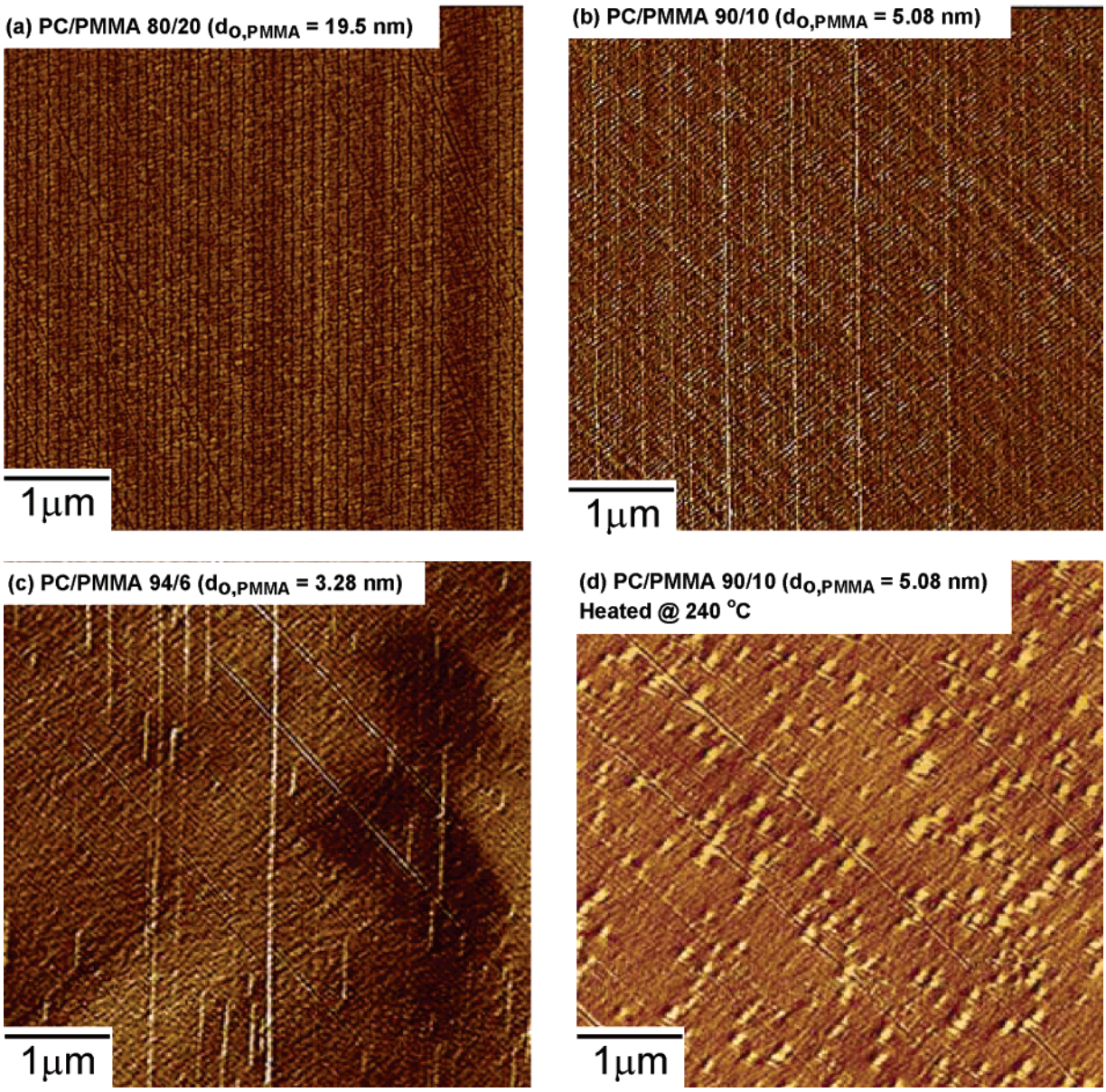

Figure 1. AFM phase images of film cross sections: (a) 100 μm thick 80/20 PC/PMMA film with $d_{0,PMMA}$ = 19.5 nm; (b) 52 μm thick 90/10 film with $d_{0,PMMA}$ = 5.08 nm; (c) 56 μm thick 94/6 PC/PMMA film with $d_{0,PMMA}$ = 3.28 μm showing layer breakup; and (d) the film in (b) after 5 min at 240 °C.

PMMA layers considerably exceeded the sum of $d_{0,PMMA}$ and $d_{0,PC}$, which indicated that some of the PMMA layers had retracted beyond the imaged area.

The persistence of continuous PMMA layers as thin as 5 nm was somewhat surprising as this dimension is considerably less than the end-to-end distance of the polymer molecule, estimated at 20−50 nm. Molecular mixing at the interphase helps to maintain layer integrity. In contrast to PMMA nanolayers, polyethylene nanolayers that were sandwiched between polystyrene layers broke up when they were as thick as 10 nm.[7] From the χ parameter, the polyethylene/styrene interphase is not as thick as the PC/PMMA interphase. Moreover, it is likely that stability of the PE nanolayer was reduced further by the onset of crystallization during cooling, which drove disentanglement of polyethylene chains from the polystyrene layers.

It is known that PMMA and PC undergo exchange reactions in the melt.[11,12] Possibly, covalent bonds, formed during the estimated 3 min of melt contact time in the layer multipliers also helped to stabilize the thin PMMA layers. This possibility is supported by reports that the delamination toughness of the PC/PMMA interphase (950 J m^{-2})[13] is somewhat higher than the delamination toughness of other polymer pairs with similar interphase thickness (less than 100 J m^{-2}).[4] On the other hand, when the films were held above the glass transition temperature at 240 °C for 5 min, interfacial-tension-driven breakup destroyed the layers and produced a dispersion of small spherical PMMA particles (Figure 1d). If there had been a high degree of exchange reaction, there would be no driving force for interfacial-tension-driven breakup. Although the extent of reaction may not be large, any covalent bonds formed at the interphase would help to maintain the integrity of the PMMA nanolayers.

Oxygen Permeability. It is possible that melt spreading and layer confinement in the layer-multiplying process resulted in some change in the constituent properties. To test this possibility, either PC or PMMA was used in both extruders, and control PC and PMMA films were extruded with the same process conditions

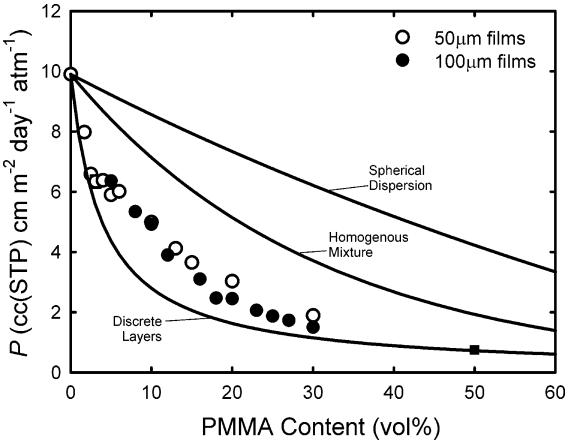

Figure 2. Oxygen permeability of 2048-layer films as a function of PMMA content. The result for a 512-layer film with 50/50 PC/PMMA composition is included as the solid square.

as the PC/PMMA films. Density and oxygen permeability did not change systematically with the film thickness or the number of layers (Table 1). It was apparent that if there was residual orientation imposed by the process, it was not enough to affect the film properties of interest in this study. Results for 50 μm films with 2048 layers served as controls values in subsequent discussions of the PC/PMMA films.

Oxygen permeability of PC/PMMA films is plotted in Figure 2 as a function of PMMA content. Because PMMA has lower oxygen permeability than PC, model calculations are especially sensitive to the morphology of the low volume fraction PMMA constituent. For reference, several model calculations are included with the experimental results as solid curves. The permeability P_d of continuous layers with perfectly sharp boundaries (discrete layers) is given as

$$P_d = \left(\frac{\phi_{0,PMMA}}{P_{PMMA}} + \frac{1-\phi_{0,PMMA}}{P_{PC}}\right)^{-1} \quad (1)$$

where P_{PMMA} and P_{PC} are the permeabilities of PMMA layers and PC layers, respectively, and $\phi_{0,PMMA}$ is the volume fraction of PMMA in the film.

The permeability of a homogeneous mixture P_h is given as

$$P_h = \exp[\phi_{0,PMMA} \ln P_{PMMA} + (1-\phi_{0,PMMA}) \ln P_{PC}] \quad (2)$$

Previous studies demonstrated that the 50/50 (v/v) composition follows the discrete layer model if the layers are thicker than about 100 nm, whereas the homogeneous mixture model closely describes completely interphase PC/PMMA materials with nominal layer thickness less than 10 nm.[3]

The predicted permeability for a spherical dispersion of less permeable PMMA particles in a more permeable PC matrix P_s is also included[14]

$$P_s = P_{PC}\left[1 + \frac{3\phi_{0,PMMA}}{\frac{(P_{PMMA}/P_{PC})+2}{(P_{PMMA}/P_{PC})-1} - \phi_{0,PMMA}}\right] \quad (3)$$

This model would describe the permeability if surface tension driven breakup completely transformed the PMMA layers into spherical particles.

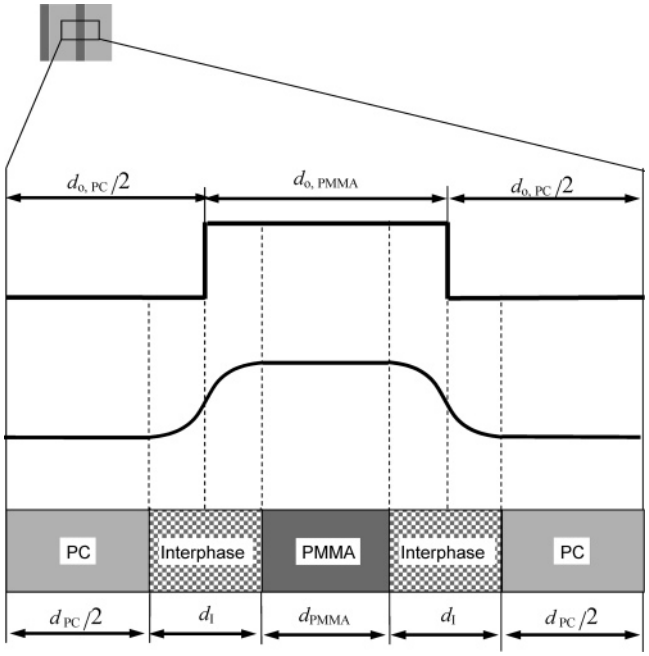

Figure 3. Schematic representation of the three-layer interphase model.

The experimental results approach the discrete layer model only if both $d_{0,PMMA}$ and $d_{0,PC}$ exceed $10d_I$, where d_I is the interphase thickness. This is exemplified by the 50/50 composition with $d_{0,PMMA} = d_{0,PC} \cong 100$ nm. As the PMMA layers become thinner, P exceeds the discrete layer value. This behavior is caused by the interphase.[3,4] Where 100 and 50 μm films overlap in composition, P of the thicker film tends to be closer to the discrete layer line. Because the number of layers is the same, the PMMA layers are proportionally thicker in the 100 μm film, and a smaller fraction of the PMMA is present as interphase. When the PMMA layers become discontinuous at very low PMMA content, P again approaches the discrete layer value. Thus, 1.7% PMMA decreases oxygen permeability of PC by 20% and 2.5% PMMA decreases it by almost 35%.

Discussion

Permeability of Continuous PMMA Layers. To describe P of films with continuous PMMA layers ($d_{0,PMMA} \geq 5$ nm) that varied in composition and layer thickness ($d_{0,PMMA} \neq d_{0,PC}$) and to obtain an estimate of the interphase thicknesses, a model of the interdiffused film is proposed in which a continuous PMMA layer of thickness d_{PMMA} is separated from PC layers of thickness d_{PC} by interphase layers of thickness d_I (Figure 3). The permeability of the layered assembly is expressed as

$$P = \left(\frac{\phi_{PMMA}}{P_{PMMA}} + \frac{\phi_{PC}}{P_{PC}} + \frac{\phi_I}{P_I}\right)^{-1} \quad (4)$$

where ϕ_{PMMA}, ϕ_{PC}, and ϕ_I are the volume fractions of the PMMA layer, the PC layer, and the PC/PMMA interphase, respectively, and P_{PMMA}, P_{PC}, and P_I are the permeabilities of PMMA, PC, and the PC/PMMA interphase. The PC/PMMA interphase permeability was determined previously and is taken as 1.62 cm^3 (STP) cm m^{-2} day^{-1} atm^{-1}.[3]

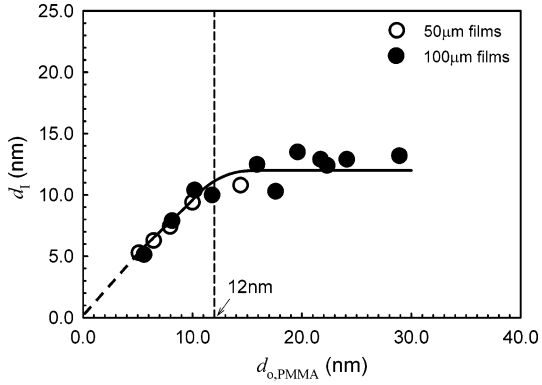

Figure 4. Relationship between interphase thickness and PMMA layer thickness.

It follows that ϕ_{PMMA}, ϕ_{PC}, and ϕ_I can be expressed separately as

$$\phi_{PMMA} = \frac{d_{PMMA}}{d_{0,PMMA} + d_{0,PC}} = \frac{d_{0,PMMA} - d_I}{d_{0,PMMA} + d_{0,PC}} \quad (5)$$

$$\phi_I = \frac{2d_I}{d_{0,PMMA} + d_{0,PC}} \quad (6)$$

$$\phi_{PC} = 1 - \phi_{PMMA} - \phi_I \quad (7)$$

where $d_{0,PMMA}$ and $d_{0,PC}$ are the nominal layer thicknesses of the PMMA layer and the PC layer. In addition

$$d_{PMMA} = d_{0,PMMA} - d_I \quad (8)$$

and

$$d_{PC} = d_{0,PC} - d_I \quad (9)$$

Equations 4−9 can be solved readily for the interphase thickness d_I and the PMMA layer thickness d_{PMMA}. The results are presented in Table 2.

The effect of $d_{0,PMMA}$ on d_I is shown in Figure 4. In this plot, results for 100 μm films and 50 μm films overlap. For $d_{0,PMMA} > 12$ nm, d_I assumes a constant value of 12 nm, which is considered the equilibrium interphase thickness. Any decrease in $d_{0,PMMA}$ is paralleled by a decrease in d_{PMMA}. A slightly lower value for d_I of 10 nm was found in a previous study of 50/50 (PC/PMMA) films.[3] The difference reflects the lower process temperature (270 °C vs 280 °C) and higher PC molecular weight (MFI = 10 vs MFI = 14) used previously. For $d_{0,PMMA} < 12$ nm, d_{PMMA} essentially vanishes and d_I is equal to $d_{0,PMMA}$. From oxygen permeability, it appears that when the PMMA layer is thinner than d_I, the interphase becomes thinner rather than more dilute in PMMA.

The results presented in Figure 4 assume uniform thickness of the PMMA layers. Because thickness variation on the order of 20% is inherent to the PC/PMMA films, the effect of layer thickness variation on P, and therefore on d_I, needs to be considered. If all the PMMA layers are thick enough to have interphase thickness of 12 nm or, on the other hand, if all the PMMA layers are thin enough that they are completely interphase, the layer distribution has no effect on P. It is only when $d_{0,PMMA}$ is close to the interphase thickness that an effect is anticipated. In this case, the thinner layers in the distribution are completely interphase, but the thicker PMMA layers are not completely interphase and some PMMA remains in the center of the layer. Because PMMA has lower P than the interphase material, a distributed layer thickness gives lower P and hence smaller apparent d_I than a uniform layer thickness.[4] Indeed, layer thickness variation may be responsible for the observed scatter in d_I when $d_{0,PMMA}$ is in the range of 12 nm (Figure 4).

The sensitivity of oxygen permeability to the interphase structure was tested with two model calculations for films with $d_{0,PMMA} < 12$ nm. Both assume that the PMMA layer is entirely taken up in the interphase. One assumes constant interphase thickness of 12 nm. The other assumes constant interphase composition of PMMA/PC 50/50. In the first model, the film is considered as an assembly of PC layers alternating with two PC/PMMA interphase layers of thickness 12 nm and variable composition depending on $d_{0,PMMA}$. The permeability P' of the assembly is expressed as

$$P' = \left(\frac{\phi_{PC}}{P_{PC}} + \frac{\phi_I}{P_I}\right)^{-1} \quad (10)$$

where ϕ_{PC} and ϕ_I are the volume fractions of PC and interphase, respectively, and P_{PC} and P_I are the permeabilities of PC and the interphase. Both the composition and permeability of the interphase depend on $d_{0,PMMA}$ in this model. It follows that

$$\phi_I = \frac{2d_I}{d_{0,PC} + d_{0,PMMA}} \quad (11)$$

and

$$\phi_{PC} = 1 - \phi_I \quad (12)$$

The composition-dependent interphase permeability can be estimated as

$$\ln P_I = V_{PMMA} \ln P_{PMMA} + (1 - V_{PMMA}) \ln P_{PC} \quad (13)$$

where V_{PMMA} is the volume fraction PMMA in the interphase layer

$$V_{PMMA} = \frac{d_{0,PMMA}}{2d_I} \quad (14)$$

with d_I taken as 12 nm. However, the reported P_I of the PC/PMMA interphase is less than the additive value from eq 13 for $V_{PMMA} = 0.5$. Therefore, the experimental P_I of the $V_{PMMA} = 0.5$ composition was used to extract an effective P_{PMMA} of 0.265 cm^3 (STP) cm m^{-2} day^{-1} atm^{-1}, and this value was used in eq 13 to obtain P_I for an interphase of composition $V_{PMMA} < 0.5$. The composite permeability based on eqs 10−14 is given in Table 2 as P'.

In the second model, films with $d_{0,PMMA} < 12$ nm are considered as an assembly of PC layers alternating with PC/PMMA interphase layers of constant composition $V_{PMMA} = 0.5$ and variable thickness depending on $d_{0,PMMA}$. The permeability of the assembly P'' is expressed as

$$P'' = \left(\frac{\phi_{PC}}{P_{PC}} + \frac{\phi_I}{P_I}\right)^{-1} \quad (15)$$

In this case, d_I is equal to $2d_{0,PMMA}$ and

$$\phi_I = \frac{2d_{0,PMMA}}{d_{0,PC} + d_{0,PMMA}} \quad (16)$$

Using the established P_I value for $V_{PMMA} = 0.5$ of 1.62 cm^3 (STP) cm m^{-2} day^{-1} atm^{-1}, the composite permeability based on eqs 15 and 16 is given in Table 2 as P''. The difference between P' and P'' is substantial, with P' being significantly higher than P''. Only P'' correlates well with the measured value of P.

It is now possible to describe what happens to the interphase as the PMMA layer thickness is decreased to the limit of layer stability, assuming uniform PMMA layers. If $d_{0,PMMA}$ is greater than 12 nm, molecular mixing creates an interphase region on either side of the PMMA layer with thickness $d_I = 12$ nm and composition PC/PMMA 50/50. This leaves a PMMA layer of thickness $d_{PMMA} = d_{0,PMMA} - d_I$. As $d_{0,PMMA}$ decreases, d_{PMMA} also decreases until it vanishes when $d_{0,PMMA} = 12$ nm, and only an interphase layer with thickness of $2d_I$ or 24 nm remains. When $d_{0,PMMA}$ is decreased below 12 nm, the PMMA is entirely consumed in an interphase region. On the basis of the correspondence between P and P'', it is concluded that the interphase region maintains the PC/PMMA 50/50 composition but is therefore reduced in thickness to $2d_{0,PMMA}$.

Permeability of Discontinuous PMMA Layers. The layer breakup seen in AFM images of films with $d_{0,PMMA} < 5$ nm suggests a structural model of PMMA domains of high aspect ratio dispersed in a PC matrix. Layer retraction and thickening result in PMMA domains with thickness on the order of 30 nm, which considerably exceeds the interphase thickness of 12 nm. It can be assumed that the increase in thickness restores the characteristic properties of PMMA to the broken layers. In particular, a continuous interphase of higher permeability is replaced by discrete PMMA domains of lower permeability. It has already been seen that the onset of layer breakup deflects the composition dependence of P toward the discrete layer relationship (see Figure 2), which is consistent with domains of relatively high aspect ratio, as seen in the AFM images.

To a first approximation, the PMMA domains ($P = 0.373$ cm^3 (STP) cm m^{-2} day^{-1} atm^{-1}) can be considered impermeable compared to PC ($P = 9.90$ cm^3 (STP) cm m^{-2} day^{-1} atm^{-1}). The Nielson model is then appropriate for analyzing P and extracting an effective aspect ratio of the PMMA domains. For a dispersion of impermeable platelets of aspect ratio α oriented perpendicular to the flux, the permeability is given as

$$P = P_0 \frac{1 - \phi}{1 + \alpha\phi/2} \quad (17)$$

where P_0 is the permeability of PC and ϕ is the volume fraction of PMMA. For films with low PMMA content, the PMMA composition determined by RI was used in the calculation. The results are summarized in Table 2. As $d_{0,PMMA}$ decreases, the aspect ratio of the broken layers increases. The exception is PC/PMMA 99/1; however, α may be unreliable because this film has the greatest uncertainty in composition. In any case, α from eq 17 should be taken as an effective aspect ratio only, in view of the wide distribution in lengths of the broken layers as seen in AFM images.

Conclusions

This study extends our use of polymer nanolayers obtained by forced assembly to probe further into the nature of the polymer interphase. In this study, the thickness of a thin PMMA nanolayer sandwiched between thicker PC layers was reduced to the limit of layer melt stability, which was determined to be about 5 nm for this polymer pair. Attempts to obtain thinner PMMA nanolayers resulted in layer breakup. Because PMMA has lower oxygen permeability than PC, the permeability was especially sensitive to the PMMA constituent in assemblies with low volume fraction PMMA.

The interphase thickness in assemblies with continuous PMMA layers was extracted from a three-layer permeability model that was adapted to PC and PMMA layers that differed in thickness. For PMMA layers thicker than 12 nm, the interphase thickness was constant and equal to 12 nm. However, for continuous PMMA layers less than 12 nm thick, the extracted interphase thickness was equal to the nominal PMMA layer thickness. On the basis of the oxygen permeability measurements, it was concluded that if the thickness of the thin PMMA nanolayer was less than the interphase thickness, the PMMA was entirely consumed in an interphase region of thickness equal to twice the nominal layer thickness. It appeared that the interphase region maintained the 50/50 average composition and therefore was reduced in thickness as the nominal PMMA layer thickness decreased.

Attempts to fabricate PMMA layers that were less than 5 nm thick resulted in layer breakup during the coextrusion process. Layer retraction and thickening resulted in PMMA domains that were much thicker than the interphase dimension. Indeed, the PMMA domains were thick enough that they appeared to have the oxygen permeability of PMMA rather than the somewhat higher oxygen permeability of the interphase. Because of the high aspect ratio of the PMMA domains, a small amount of PMMA significantly reduced the oxygen permeability of the continuous PC phase. Thus, 1.7% and 2.5% PMMA decreased permeability of PC by 20% and 35%, respectively.

Acknowledgment. This research was generously support by NSF (Grant DMR-0349436).

References and Notes

(1) Merfeld, G. D.; Paul, D. R. In *Polymer Blends*; Paul, D. R., Bucknall, C. B., Eds.; Wiley: New York, 2000; Vol. 1, pp 55 ff.

(2) Farinha, J. P. S.; Vorobyova, O.; Winnik, M. A. *Macromolecules* **2000**, *33*, 5863−5873.

(3) Liu, R. Y. F.; Jin, Y.; Hiltner, A.; Baer, E. *Macromol. Rapid Commun.* **2003**, *24*, 943−948.

(4) Liu, R. Y. F.; Bernal-Lara, T. E.; Hiltner, A.; Baer, E. *Macromolecules* **2004**, *37*, 6972−6979.

(5) Liu, R. Y. F.; Bernal-Lara, T. E.; Hiltner, A.; Baer, E. *Macromolecules* **2005**, *38*, 4819−4827.

(6) Jin, Y.; Rogunova, M.; Hiltner, A.; Baer, E.; Nowacki, R.; Galeski, A.; Piorkowska, E. *J. Polym. Sci., Part B: Polym. Phys.* **2004**, *42*, 3380−3396.

(7) Bernal-Lara, T. E.; Liu, R. Y. F.; Hiltner, A.; Baer, E. *Polymer* **2005**, *46*, 3043−3055.

(8) Baer, E.; Kerns, J.; Hiltner, A. In *Structure Development During Polymer Processing*; Cunha, A. M., Fakirov, S., Eds.; Kluwer Academic Publishers: Dordrecht, 2000; pp 327−344.

(9) Mueller, C.; Kerns, J.; Ebeling, T.; Nazarenko, S.; Hiltner, A.; Baer, E. In *Polymer Process Engineering 97*; Coates, P. D., Ed.; Institute of Materials: London, 1997; pp 137−157.
(10) Sekelik, D. J.; Stepanov, S. V.; Nazarenko, S.; Schiraldi, D.; Hiltner, A.; Baer, E. *J. Polym. Sci., Part B: Polym. Phys.* **1999**, *37*, 847−857.
(11) Rabeony, M.; Hsieh, D. T.; Garner, R. T.; Peiffer, G. *J. Chem. Phys.* **1992**, *97*, 4505−4511.
(12) Landry, C. J. T.; Henrichs, P. M. *Macromolecules* **1989**, *22*, 2157−2166.
(13) Kerns, J.; Hsieh, A.; Hiltner, A.; Baer, E. *J. Appl. Polym. Sci.* **2000**, *77*, 1545−1557.
(14) Petropoulos, J. H. *Adv. Polym. Sci.* **1985**, *64*, 93−143.

MA051649X